Experimental and Numerical Studies of Sheet Electron Beam Propagation through a Planar Wiggler Magnet

Ze-Xiang Zhang, Victor L. Granatstein, *Fellow, IEEE*, W. W. Destler, *Fellow, IEEE*, Steven W. Bidwell, J. Rodgers, S. Cheng, T. M. Antonsen, Jr., *Member, IEEE*, B. Levush, *Senior Member, IEEE*, and D. J. Radack *Member, IEEE*

Abstract—**Detailed experimental studies on sheet relativistic electron beam propagation through a long planar wiggler are reported and compared with numerical simulations. The planar wiggler has 56 periods with a period of 9.6 mm. Typically, the wiggler field peak amplitude is 5 kG. The experimental efforts have been focused on control of the deviation of the beam toward the side edge of the planar wiggler along the wide transverse direction. It is found that a suitably tapered magnetic field configuration at the wiggler entrance can considerably reduce the rate of the deviation. The effects of the following techniques on beam transport efficiency are also discussed: side focusing, beam transverse velocity tuning at the wiggler entrance, and beam spread limiting. High beam transport efficiency (almost 100%) of a 15 A beam has been obtained in some cases. The results are relevant to development of a free electron laser amplifier for application to stabilizing and heating of plasma in magnetic fusion research.**

I. Introduction

THE CONCEPT of a planar wiggler [1] sheet beam FEL amplifier [2] in the millimeter wavelength range was put forward several years ago and its operating parameters were defined based on one-dimensional calculations [3] as: beam energy 470 keV, beam current 10 A, wiggler period 9.6 mm, wave frequency 94 GHz, waveguide size 40 mm by 3.2 mm, and wiggler magnetic field amplitude 5.0 kG. As a first step a planar wiggler with 56 periods was built to demonstrate the principles of this kind of FEL amplifier.

A recent three-dimensional FEL amplifier simulation [4], which takes practical imperfections (wiggler magnetic field amplitude fluctuation and beam transverse velocity spread at the entrance of the wiggler) into account, has shown that there is a wiggler field threshold (4.5 kG) and a beam current threshold (2 A) for the 56-period system to achieve amplification. The power gain increases when the strength of the wiggler magnetic field increases until a saturation field strength is reached. The power gain is found very sensitive to the beam current. To get a power amplification of 10 dB the wiggler magnetic field amplitude must be higher than 4.5 kG and the beam current must be higher than 5A. Thus, to achieve significant amplification in the FEL amplifier it is important to achieve sufficient beam current transport through the entire wiggler (56 periods) at high magnetic field.

An experiment on sheet beam propagation through a planar wiggler was reported and analyzed previously [5]; the planar wiggler was shown to have a beneficial focusing effect in the small transverse direction of the sheet beam. The wiggler used in that experiment had 10 periods and it produced a wiggler magnetic field with an amplitude of 2 kG.

With a longer wiggler and a stronger field some new problems were encountered. First, the beam spread must be limited more critically. Second, the magnetic field configuration at the beam entrance was found to be critically important to beam transport efficiency; a suitable field entrance taper is essential to ensure high beam transport efficiency. Also, some side focusing mechanism is required to suppress beam loss out the side edge of the planar wiggler along the wide transverse direction of the sheet beam. Finally, the magnetic material in the wiggler must not be saturated if high fields are to be obtained.

Several methods of creating an appropriate wiggler field entrance taper and several taper configurations were tested. A side focusing concept was developed; however, it was not completely effective in high field experiments due to the fact that the wiggler is close to saturation. When the field entrance taper is optimized, however, almost 100% beam transport efficiency has been achieved at high magnetic field values for beams with limited moderate widths.

A numerical simulation study of sheet beam propagation through a planar wiggler has been completed and will be described in Section III. In the simulation, some practical imperfections of the system were included: the wiggler magnetic field amplitude had a fluctuation of 2.5% and this fluctuation is randomly applied from peak to peak; the sheet beam had transverse velocity components and these components are randomly distributed; finally, beam energy spread was allowed for. Note that the code de-

Manuscript received May 12, 1993; revised July 12, 1993. This work was supported by the U.S. Department of Energy.

Z.-X. Zhang, V. L. Granatstein, W. W. Destler, J. Rodgers, S. Cheng, T. M. Antonsen, Jr., and B. Levush are with the University of Maryland, College Park, MD 20742-3511.

S. W. Bidwell is with the NASA/Goddard Space Flight Center, Greenbelt, MD 20771.

D. J. Radack is with SAIC, Arlington, VA.

IEEE Log Number 9213489.

scribed in Section III is only a propagation code without including the radiation field. In contrast, the evolution of the radiation field was simulated in [4] which also gave traces of sample electrons. The traces given by the two codes were the same within the considered power level up to 200 kW.

The experimental results have been compared with the numerical simulations and qualitative agreement, and in some cases quantitative agreement was found.

II. Experimental Results

The basic experimental configuration is shown in Fig. 1. The electron beam was generated from a cold cathode by explosive field emission. The planar cathode had a velvet emitting surface. The anode consisted of two plates with a slot in each plate through which the beam passes. The distance between the two anode plates was 40 mm. The short dimension of the slots was 1.0 mm and the long dimension was changeable from shot to shot. This kind of anode structure is referred to as a two-slot anode. The beam spread angle and transverse velocity spread could be limited by the two slot anode. Actually only the beam spread angle along the small transverse direction was limited by the anode to 1.4°. The beam spread angle along the small transverse direction was not limited by the anode, because the anode limited beam spread angle along that direction would be 26.6° at a slot width of 20 mm, but the real spread angle along that direction was less than 10°, estimated based on indirect measurement. The cathode-anode distance was 14 mm in most of the cases studied. The wiggler had 56 periods with a periodicity of 9.6 mm and the gap between the two halves of the wiggler formed the channel for beam passage. This gap had transverse dimensions of 59 mm by 3.2 mm (the wide transverse dimension of the gap was limited by the supporting structure of the windings of the wiggler). In planned FEL amplifier experiments, an amplifier waveguide will be placed in this gap. Behind the second plate of the two-slot anode was a miter bend which acts as a beam-wave injection coupler.

We tested two different types of miter bend. The first was a hole miter bend with a linear array of holes through the miter bend which functions as a beam channel. The second was a mesh (screen) miter bend. The first had a beam transparency of 45% and a RF reflectivity of 95%. The second had a beam transparency of 95% but a RF reflectivity of only 45%. The beam current recorded at the exit of the wiggler was almost the same for these two miter bends if other parameters were the same, but the beam current at the entrance of the wiggler (just behind the miter bend) for the case of the mesh miter bend was twice of that for the case of the hole miter bend. In this paper whenever a miter bend is mentioned, it is the hole miter bend.

The accelerating voltage for the beam was produced by a high voltage pulse generator shaped by a water pulse forming line (PFL). The duration of the pulse was 100 ns

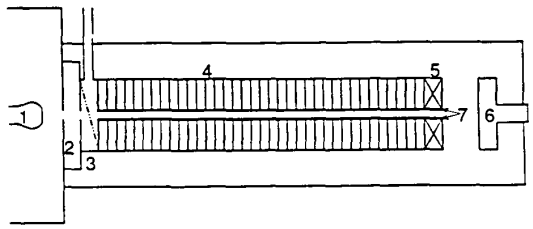

Fig. 1. Experimental setup for sheet beam propagation studies (not in scale). (1) cathode. (2) anode. (3) miter bend. (4) wiggler, 56 periods, with a period of 9.6 mm. (5) Pokofski coil. (6) Faraday cup. (7) amplifier waveguide. The dimension of the figure is not in scale with the real experimental setup.

and the beam energy (cathode voltage) in most of these propagation experiments was 470 keV $\pm$ 5 keV. The wiggler magnet was driven by a pulse power supply consisting of an electrolytic capacitor bank, with a capacitance of 0.12 F. The wiggler magnetic field amplitude produced by this power supply as a function of wiggler current is shown in Fig. 2.

A Faraday cup was used to monitor the beam current. To determine the beam propagation efficiency under certain conditions, the Faraday cup was initially placed just behind the anode and data was taken for five or more shots. The averaged recorded beam current was taken as the injection current to the wiggler. The wiggler was then inserted in position and the Faraday cup was placed just at the exit of the wiggler and data was again obtained for several shots. The averaged recorded beam current was then taken as the transported current. Data on beam transport efficiency was obtained from these measurements. The beam current typically has 10% fluctuation from shot to shot even when all experimental parameters were held unchanged.

In some experiments a Cerenkov witness plate was set in the beam channel to observe the beam crosssection. This plate is a transparent piece of plastic covered by graphite powder on its upstream surface. A time integrated photograph of the plate indicates the beam crosssection. Experimental results are summarized below.

A. The Effect of Magnetic Field Entrance Taper on Transport Efficiency

Since numerical simulations showed the critical importance of the wiggler magnetic field configuration at the beam entrance to beam transport, a method of constructing different wiggler field entrance tapers was required. Two methods were used to construct the entrance taper. One method was to use an additional short section of wiggler consisting of permanent magnetic pieces. Another method involved the use of current shunt pieces in the first few periods of the wiggler winding and adjustment of the thickness of the magnetic pole pieces in the slots of the first few periods of the wiggler winding. Both types of entrance taper were constructed. The taper made of permanent magnets was not uniform in periodicity, especially at the connection between the taper and the main

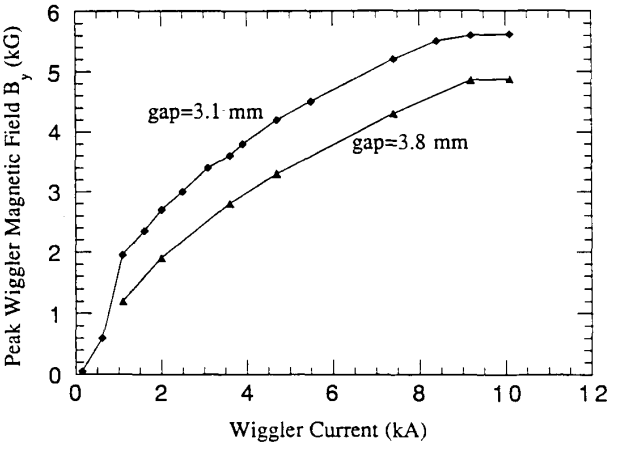

Fig. 2. Peak wiggler magnetic field strength versus wiggler current for different gap dimensions.

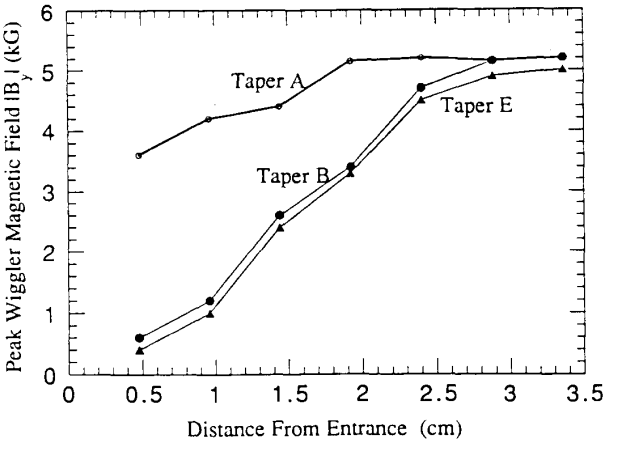

Fig. 3. Absolute values of the peak wiggler magnetic fields of the first seven half periods under three different entrance taper configurations. Neighboring peak fields have opposite polarity to each other.

body of the wiggler, thus the beam propagation efficiency obtained by this taper was not so good as that obtained by the other taper. The entrance taper used in the study described in this paper was produced by the second method. This method has the disadvantage that an optimized field configuration is achieved only at a particular wiggler current. If the wiggler field amplitude following the taper is to be changed, the entrance taper must be adjusted as well. In contrast the taper configuration created by the first method (permanent magnets) can be adjusted more easily. If the problem matching the taper to the main body of the wiggler (keeping uniform periodicity and magnetic field continuity) could be solved this method would be a good approach. Typical entrance tapers used in the experiments are shown in Fig. 3.

The following experiments were performed with a beam width of 40 mm. There was no miter bend behind the two slot anode and no waveguide in the wiggler gap, so that the beam channel was 59 mm by 3.2 mm. Two taper configurations were compared: taper A and taper B (see Fig. 3). Under taper A the beam transport efficiency is only 6% at 5 kG peak wiggler field. Under taper B the beam transport efficiency is 44% at 5 kG.

It is evident that the magnetic field entrance taper plays a very important role in beam propagation. The optimum taper configuration studied was the taper E in Fig. 3. With this taper configuration, the beam transport efficiency was 50% for a beam with a width of 40 mm, and almost 100% beam transport efficiency was obtained for a beam with a width of 20 mm. These experiments were carried out in the case of without the miter bend and without the waveguide.

The beam transport efficiency measured for these different tapers under low magnetic fields (up to 3 kG) is not as strongly different as in the high magnetic field cases due to the fact that, the entrance taper configurations are actually much less different from each other in the low magnetic field cases.

The explanation for the effect of the entrance taper on beam propagation is the following. The electrons tend to deviate toward the side edge of the planar wiggler along the wide transverse direction of the sheet beam while propagating through the planar wiggler. We observed the deviation by Cerenkov witness plate photograph. This kind of deviation is an essential tendency of motion of electrons in a planar wiggler as a result of constant canonical momentum in that direction, because the magnetic field of the planar wiggler is independent of the wide transverse dimension (except at the very edge of the wiggler). An optimum magnetic field taper at the entrance can considerably reduce the rate of such deviation. Our numerical simulations have confirmed this explanation (see next section and compare Fig. 5 to Fig. 6).

B. The Effect of an Offset of the Wiggler Magnetic Pole Pieces on Transport Efficiency

Neighboring magnetic pole pieces in the wiggler could be set with a relative displacement or offset to each other along the wide transverse direction of the sheet beam. This offset produced a net dc magnetic field component at both side edges of the wiggler with opposite polarity on each side. If with a given wiggler current direction the dc magnetic field component turned the beam toward the center part of the wiggler, then, when the wiggler current direction was reversed, a defocusing effect could be expected.

Experiments were carried out for a net offset of 2.0 mm, 3.5 mm, 5.0 mm, and 7.5 mm. In the 3.5 mm case and the 5.0 mm case better results were obtained than in the 2.0 mm case or 7.5 mm case. The experimental results described below are in the 3.5 mm case. The two-slot anode structure was used in these experiments with a slot width of 20 mm and with the miter bend behind the anode (it was observed that the installation of the miter bend always reduced the propagation efficiency). The cathode-anode gap was 14 mm. Polarity A and polarity B will be

used to denote the two opposite wiggler current directions. For a wiggler magnetic field amplitude of 3.0 kG, the beam transport efficiency was 93% in polarity B (the "focusing" polarity) and was only about 15% in polarity A (the "defocusing" polarity). For a wiggler magnetic field amplitude of 4.9 kG, the beam transport efficiency was 80% in polarity B and was 73% in polarity A. In these experiments the wiggler field entrance taper was close to the optimized entrance taper, taper E, which is shown in Fig. 3.

We see that in the lower wiggler field case the offset made a great difference to beam transport efficiency under different wiggler current polarities. However, in the higher wiggler field case, the offset did not make a large difference to beam transport efficiency between different wiggler current polarities. The result is due to the fact that the wiggler is close to saturation under high field operation. This fact can also be seen from Fig. 2.

If a waveguide is inserted into the wiggler gap for FEL amplifier experiments, the wiggler gap must be further increased (because for beam energy 470 keV, wiggler magnetic field 5.0 kG, wave frequency 94 GHz at TE_{01} mode, the small transverse dimension of the waveguide must be 3.2 mm, the gap size must be this dimension plus the thickness of the wall of the waveguide). In this case the wiggler current must be increased as well to obtain the same magnetic field strength in the gap. The wiggler will then be more deeply saturated under high field operation. In that case, an alternative side focusing method should be found to improve the beam propagation efficiency. Another approach could be to construct a waveguide which is very thin in the small transverse direction, but this would result in increasing the beam energy (for example, if the small transverse dimension of the waveguide is 2.6 mm, the wiggler magnetic field is 5.0 kG, and the wave frequency is 94 GHz at TE_{01} mode, the resonant beam energy becomes 696 keV). The best approach may be to make improvements in the design of the wiggler itself to avoid the saturation effect.

C. The Effect of Beam Width on Transport Efficiency

The effect of beam width on transport efficiency has also been studied. Different beam widths were obtained by changing the width of the anode slots. The experimental result are shown in Fig. 4.

From Fig. 4, it is evident that almost 100% beam transport efficiency was obtained for beams with a width less than 20 mm.

The explanation for this experimental result is as follows. There were some electrons at the edges of the beam with a short distance from the side wall of the channel. In the experimental condition all electrons in the sheet beam deviated toward one side wall of the channel, while propagating through the wiggler gap, with a drift velocity which can be found approximately from (4) in the next section. Those electrons located at the unfavorite edge may strike the side wall before reaching the exit of the wiggler. The wider the sheet beam, the higher the percentage of such wall-striking electrons.

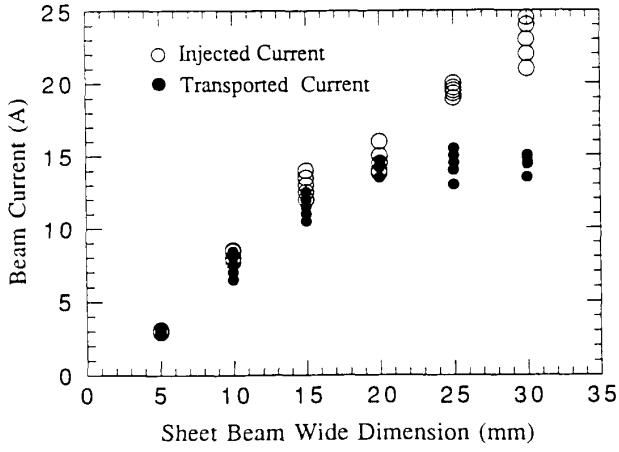

Fig. 4. Transported beam current versus beam width under taper E (shown on Fig. 3).

D. Summary

Some experimental results (under 5 kG) mentioned in this section are summarized in Table I. Note that the beam propagation efficiency through the whole channel (54 cm) was always zero in any case we tested if no wiggler magnetic field was supplied.

III. Numerical Simulations

In this section results of numerical studies of sheet beam propagation through a planar wiggler are presented. A group of electrons (600 sample electrons used in the simulation) with random velocity spread and random energy spread were considered. Also, the wiggler model was assumed to have random magnetic field amplitude fluctuations from peak to peak.

The equation of motion of a single electron in a magnetic field is

$$m\gamma \frac{d\vec{v}}{dt} = e\vec{v} \times \vec{B} \tag{1}$$

where γ is the relativistic factor of the electron, m is its rest mass. The wiggler magnetic field for a planar wiggler was derived in [2]. For a very thin sheet beam, we can get a zero order approximation solution for the trace projection on the x-z plane by assuming all electrons at the $y = 0$ plane. Here z is the axial direction, x is the wide transverse direction of the sheet beam, and y is the short transverse direction. At the $y = 0$ plane we have

$$B_z = 0, \text{ and} \tag{2a}$$

$$B_y = B_0 \sin (k_w z) \tag{2b}$$

where $k_w = 2\pi/\lambda_w$ is the wave number of the wiggler magnetic field. In this case, the velocity component v_x

TABLE I
SUMMARY OF PROPAGATION EXPERIMENTS (5 kG)

Taper	Channel Size	Beam Size	Miter Bend	Efficiency
E	59 mm by 3.2 mm	40 mm by 1.0 mm	Without	50%
E	59 mm by 3.2 mm	20 mm by 1.0 mm	Without	100%
E	59 mm by 3.2 mm	20 mm by 1.0 mm	With	80%
B	59 mm by 3.2 mm	40 mm by 1.0 mm	Without	44%
A	59 mm by 3.2 mm	40 mm by 1.0 mm	Without	6%

may be separated from other components to obtain

$$\frac{dv_x}{dz} = \frac{|e|}{m\gamma} B_0 \sin(k_w z). \tag{3}$$

This equation has the solution

$$x(z) = x_0 + \left(\frac{v_{x0}}{v_z} + \frac{|e|B_0}{m\gamma k_w v_z}\right) z - \frac{|e|B_0}{m\gamma k_w^2 v_z} \sin(k_w z) \tag{4}$$

where v_{x0} is the transverse velocity component of the electron along the x direction at the entrance, v_z is the velocity component of the electron along the axial direction and is assumed independent of z, x_0 is the coordinate of the electron at the entrance.

The second term (the term in the parentheses) in (4) is usually the dominant term, and the third term (the last term) is usually much smaller than the second term. From (4), it is evident that the trace projection on the x-z plane is a linear deviation, together with a small amplitude oscillation. It is also clear that if v_{x0} can be adjusted so that the second term disappears, the deviation of the electron in the x direction can be diminished. This technique is referred to as transverse velocity tuning. For a real electron beam the transverse velocity tuning will not be very effective in improving beam transport efficiency unless the transverse velocity spread of the electrons in the beam is very small.

Other possible techniques for controlling this kind of deviation include magnetic field tapering at the entrance and side focusing. Both of these approaches have been studied experimentally. The effects of magnetic field tapering will be shown numerically below.

Now a description of our numerical model is presented. The field peak value of the kth half period of the wiggler is assumed to be:

$$B_0^{(k)} = B_0(1 + B_{dis} \times R_k^{(b)}) \tag{5}$$

where $R_k^{(b)}$ is a random number with a Gaussian distribution in $[-1, 1]$, B_{dis} is the parameter of field spread, which is set to be 0.025 in this simulation based on our measurements.

The energy of the jth electron is assumed to be:

$$E_j = E_0(1 + E_{dis} \times R_j^{(e)}) \tag{6}$$

where $R_j^{(e)}$ is a random number with Gaussian distribution in $[-1, 1]$, E_{dis} is the parameter of beam energy spread, which is set to be 0.03 in this simulation, based on the measured accelerating voltage waveform.

The initial transverse velocity of the jth electron is assumed to be

$$v_x^{(j)}/v_z^{(j)} = \alpha_x \times R_j^{(x)} \tag{7a}$$

$$v_y^{(j)}/v_z^{(j)} = \alpha_y \times R_j^{(y)} \tag{7b}$$

where $R_j^{(x)}$ and $R_j^{(y)}$ are random numbers with Gaussian distribution in $[-1, 1]$, and α_x and α_y are parameters of transverse velocity spread.

The wiggler model is a 2-D planar wiggler model. It was determined that such a model closely approximates the measured field distribution, except at the very edge of the wiggler. The formulas used in the code for the wiggler magnet field components are

$$B_z = B_0^{(k)} f(z) \sinh(k_w y) \cos(k_w z) \tag{8a}$$

$$B_x = 0 \tag{8b}$$

$$B_y = B_0^{(k)} f(z) \cosh(k_w y) \sin(k_w z) \tag{8c}$$

where $B_0^{(k)}$ is given by (5), which varies from half period to half period. $f(z)$ determines the tapering rule and the rule used is

$$f(z) = \sin^2(k_w z/4N_{tap}) \tag{9a}$$

when $0 \le z \le N_{tap}\lambda_w$ and

$$f(z) = 1 \tag{9b}$$

when $z > N_{tap}\lambda_w$, where N_{tap} is the number of periods of the entrance taper. This rule is close to the taper E configuration when N_{tap} is equal to 3.

The equations to describe the electron motion are

$$dx/dz = v_x/v_z, \tag{10a}$$

$$dy/dz = v_y/v_z, \tag{10b}$$

$$dv_x/dz = (e/m/(v_z\gamma))(v_y B_z - v_z B_y), \tag{10c}$$

$$dv_y/dz = (e/m/(v_z\gamma))(v_z B_x - v_x B_z), \text{ and} \tag{10d}$$

$$dv_z/dz = (e/m/(v_z\gamma))(v_x B_y - v_y B_x). \tag{10e}$$

For each particle these five equations are solved, together with the corresponding initial conditions for each electron. Coupling between electrons (self electric fields) is not considered because the current density is small. The wiggler has 56 periods with a periodicity of 9.6 mm. The main simulation results are summarized below.

In most cases, the amplitude of the betatron motion of electrons in the short transverse direction of the sheet beam is limited to small values by the wiggler, and the period of this betatron oscillation is dependent on the strength of the wiggler magnetic field. The electrons are also seen to deviate toward the side wall of the wiggler channel along the wide transverse direction of the beam; see Fig. 5 (bottom). In this case the wiggler magnetic field was not tapered at the entrance. From Fig. 5 we see that the sample electron deviates toward the side a distance of 21 cm as it propagates 54 cm along the z-direction.

Fig. 6 shows the projection of the orbit of a sample electron on y-z plane (top) and on x-z plane (bottom) for a case with entrance taper ($N_{tap} = 2$). The other parameters used in this simulation are the same as those used in the Fig. 5 case. It is now seen that the deviation along x-direction is reduced from 21 cm to 2.8 cm.

We see that the speed of the deviation along the wide transverse direction can be suppressed by a suitably selected entrance taper configuration. As a result, the beam transport efficiency is sensitive to the magnetic field entrance taper configuration. Fig. 7 shows the calculated results for $N_{tap} = 0$, 1, 3, and 5. It is evident from Fig. 7 that a slowly rising taper configuration is required to obtain high beam transport efficiency. The taper E described before is a three-period taper. We did not succeed in obtaining a longer taper with a uniform periodicity.

Another simulation shows the relation between the beam transport efficiency and the beam transverse velocity spread. In these calculations the channel dimensions were 59 mm by 3.2 mm and the initial beam size was 20 mm by 1.0 mm. The wiggler magnetic field amplitude was 0.5 T and its fluctuation parameter, B_{dis}, was 0.025. The beam energy parameter, E_O, was 470 keV. The beam energy spread parameter, E_{dis}, was 0.03. The parameter for describing the spread of the transverse velocity along the short transverse direction, α_y, was 0.03. The beam transport efficiency as a function of α_x, the parameter of transverse velocity spread along the wide transverse direction of the beam, is shown in Table II for $N_{tap} = 3$. This result suggests that the beam transverse velocity spread along the wide transverse direction should be controlled within a very small extent in order to obtain high beam transport efficiency even if the wiggler is tapered at the beam entrance.

The effect of the beam width to propagation efficiency was also simulated. The following parameters were used in this simulation: $B_0 = 0.5$ T, $B_{dis} = 0.02$, $E_0 = 470$ keV, $E_{dis} = 0.005$, $\alpha_x = 0.01$, $\alpha_y = 0.01$, and $N_{tap} = 3$. The results are shown in Table III.

The numerical simulation data for the beam width of 40 mm is not in agreement with the experimental data. If we assume that the beam spread is also changed when the beam width is changed we can get a consistent result. Using $E_{dis} = 003$, $\alpha_x = 0.2$, $B_{dis} = 0.025$, and keeping all other parameters not changed, the code gave a 48% propagation efficiency for a beam width of 40 mm.

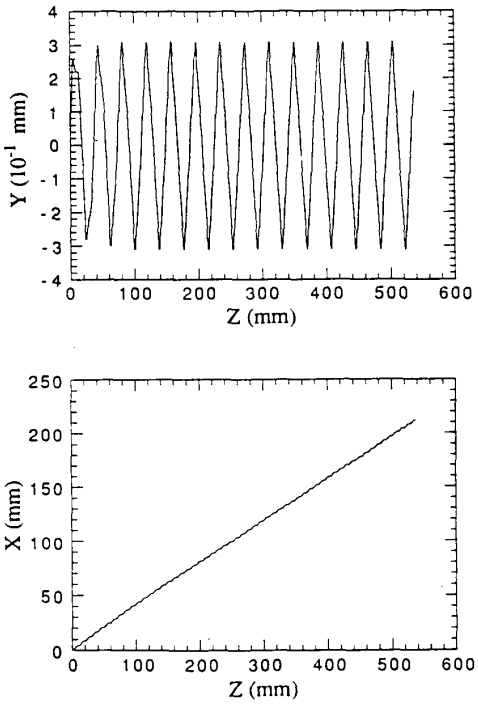

Fig. 5. Projection of the orbit of a sample electron on y-z plane (top) and on x-z plane (bottom) for the case of $N_{tap} = 0$, $E_0 = 470$ keV, $v_{x0}/v_{z0} = 0.10$, $v_{y0}/v_{z0} = 0.05$, $x_0 = 0.0$, $y_0 = 0.0$, $B_0 = 5.0$ kG, and $B_{dis} = 0$.

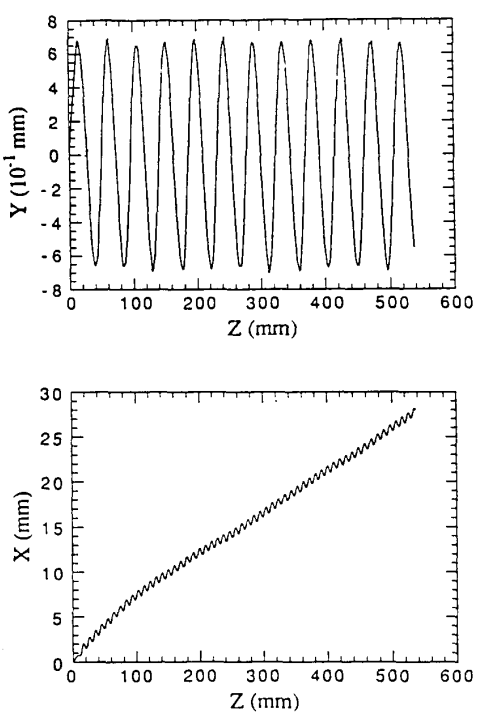

Fig. 6. Projection of the orbit of a sample electron on y-z plane (top) and on x-z plane (bottom) for the case of $N_{tap} = 2$, $E_0 = 470$ keV, $v_{x0}/v_{z0} = 0.10$, $v_{y0}/v_{z0} = 0.05$, $x_0 = 0.0$, $y_0 = 0.0$, $B_0 = 5.0$ kG, and $B_{dis} = 0$.

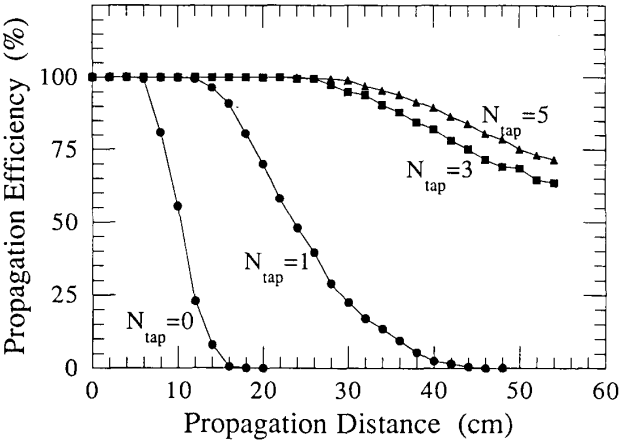

Fig. 7. Propagation efficiency as a function of propagation distance under different taper "steepness," with B_0 = 5.0 kG, B_{dis} = 0.025, E_O = 470 keV, E_{dis} = 0.005, α_x = 0.10, α_y = 0.05, beam dimensions 20 mm by 1.0 mm, and channel dimensions 59 mm by 3.2 mm.

TABLE II
TRANSPORT EFFICIENCY VERSUS α_x

α_x	0.00	0.03	0.05	0.10	0.20
Efficiency	90%	87%	76.5%	64%	51%

TABLE III
TRANSPORT EFFICIENCY VERSUS BEAM WIDTH

Beam Width	20 mm	30 mm	40 mm
Efficiency	99%	88%	79%

IV. CONCLUSION

Propagation of a sheet electron beam through a long planar wiggler (56 periods) under high wiggler magnetic field conditions has been studied in detail experimentally and numerically. Almost 100% transport efficiency through a 56-period wiggler at 5 kG has been obtained for a sheet beam with dimensions 20 mm by 1.0 mm and a wiggler channel size 59 mm by 3.2 mm. It has been confirmed that to ensure high beam transport efficiency the wiggler magnetic field must be tapered at the beam entrance and the beam energy and velocity spread must be limited. For a wide sheet beam some kind of side focusing or particle transverse velocity tuning is also required to control the essential deviation of the beam toward the side edge of the planar wiggler.

ACKNOWLEDGMENT

The authors wish to thank J. Pyle, K. Diller, and D. Cohen for their valuable technical assistance. This research was supported in part by the Department of Energy.

REFERENCES

[1] V. L. Granatstein, W. W. Destler, and I. D. Mayergoyz, "Small-period electromagnet wigglers for free electron lasers," *Appl. Phys. Lett.*, vol. 47, no. 6, pp. 643–645, Sep. 1985.

[2] W. W. Destler, V. L. Granatstein, I. D. Mayergoyz, and Z. Segalov, "Near-millimeter free electron laser designs based on measured characteristics of small-period electromagnet wigglers," *J. Appl. Phys.*, vol. 60, no. 2, pp. 521–528, July 1986.

[3] A. Serbeto, B. Levush, and T. M. Antonsen, Jr., "Efficiency optimization for free electron laser oscillators," *Phys. Fluids*, vol. B1, no. 2, pp. 435–439, Feb. 1989.

[4] Z. X. Zhang, S. W. Bidwell, H. P. Freund, V. L. Granatstein, and B. Levush, "Numerical study of a sheet beam planar wiggler free electron laser amplifier," Laboratory for Plasma Research, University of Maryland, College Park, MD, CPB (Charged Particle Beam) Tech. Rep. #92-008.

[5] J. H. Booske, W. W. Destler, Z. Segalov, D. J. Radack, E. T. Rosenbury, J. Rodgers, T. M. Antonsen, Jr., V. L. Granatstein, and I. D. Mayergoyz, "Propagation of wiggler focused relativistic sheet electron beams," *J. Appl. Phys.*, vol. 64, no. 1, pp. 6–11, July 1988.

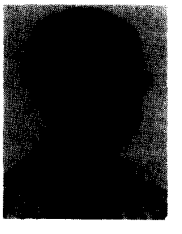

Ze-Xiang Zhang received the B.S. degree in physics from the Nan-Kei University, China in 1964, the M.S. degree in physics from the Institute of Physics, Academia Sinica, China in 1968 and the Ph.D. degree in electrical engineering from the University of Maryland in 1993.

From 1968 to 1980 and from 1984 to 1985 he was with the Institute of Physics, Academia Sinica, working with plasma physics and nuclear fusion. He was one of the main investigators who designed and operated China's first Tokamak CT-6. His research fields were power supply engineering, electromagnetic diagnostics, feed-back plasma column equilibrium control, and ECRH. From 1981 to 1983 he was with the IPP, Garching, Germany, and in the University of Stuttgart, Germany as an Alexander von Humboldt scholar, working with ECRH engineering and simulations. From 1986 to 1988 he was with the Central Nationalities College, Beijing, giving lectures on numerical analysis and computer languages. From May 1988 to the present he has been working in the Laboratory for Plasma Research, University of Maryland, involved in the sheet beam short period planar wiggler free electron laser project. He completed the proof-of-principle experiment for this kind of FEL amplifier. His recent research interests are in FEL's and high power microwave sources.

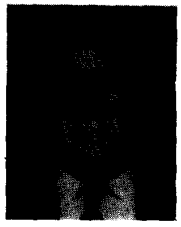

Victor L. Granatstein (S'59-M'64-SM'86-F'92) received the Ph.D. degree in Electrical Engineering and Plasma Physics in 1963 from Columbia University.

After a year of post-doctoral work at Columbia, he was a member of the Technical Staff, Bell Telephone Laboratories from 1964-1972. From 1969-1970, he was a Visiting Senior Lecturer at the Hebrew University of Jerusalem. In 1972 he joined the Naval Research Laboratory as a Research Physicist and from 1978 to 1983 he served as Head of the High Power Electromagnetic Radiation Branch. In August 1983, he became a Professor in the Electrical Engineering Department at the University of Maryland. He is presently leading experimental and theoretical studies of electromagnetic radiation from relativistic electron beams, advanced concepts in millimeter-wave tubes, free electron lasers, and gyroton amplifiers. He is a Fellow of the American Physical Society. He is Associate Editor of the *International Journal of Electronics*, and has been a guest editor of the *IEEE Transactions on Microwave Theory and Technique* and the *IEEE Journal of Quantum Electronics*. He has been a reviewer for NSF, AFOSR, DoE DNA, ONR, and ARO. He has co-authored more than 150 research papers in regular journals, and holds a number of patents on active and passive microwave devices.

Dr. Granatstein's awards include the E.O. Hulburt Annual Science Award for 1979, the Superior Civilian Service Award (1980), the Conrad Award for Scientific achievement (presented by the Secretary of the Navy in 1981), the IEEE Plasma Science and Application Award (1991), and a Fulbright Senior Scholar Award (1993). Since 1988, he has been Director of the Institute for Plasma Research at the University of Maryland.

W. W. Destler, photograph and biography not available at the time of publication.

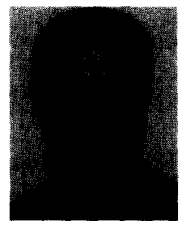

Steven W. Bidwell was born in Highland Park, MI in 1961. He received the Ph.D. degree in nuclear engineering from the University of Michigan in 1989. His doctoral research examined the interaction of intense relativistic electron beams with flames and gases. At the University of Maryland's Laboratory for Plasma Research he pursued free-electron laser research using intense relativistic electron beams for the generation of high power millimeter-wave radiation.

He is currently employed with the NASA/Goddard Space Flight Center in Greenbelt, MD. Since August 1992 he has been with Goddard's Laboratory for Hydrospheric Processes where he is developing microwave techniques for remote sensing of the environment. Presently he is developing an airborne X-band Doppler radar for the study of thunderstorms and mesoscale convective weather systems.

J. Rodgers, photograph and biography not available at the time of publication.

S. Cheng, photograph and biography not available at the time of publication.

T. M. Antonsen, photograph and biography not available at the time of publication.

B. Levush, photograph and biography not available at the time of publication.

D. J. Radack, photograph and biography not available at the time of publication.